JOURNAL OF APPLIED ELECTROCHEMISTRY 23 (1993) 435–442

Joule heating induced local electrodeposition for microelectronic circuits*

H. KAWAMOTO

Manufacturing Engineering Research Laboratory, Corporate Research Laboratories, Fuji Xerox Co., Ltd 2274, Hongo, Ebina-shi, Kanagawa 243-04, Japan

Received 15 June 1992; revised 5 November 1992

A fundamental study is performed for local electrodeposition of copper utilizing thermal potential induced by Joule heating. The feasibility of the process for microelectronic applications is assessed by both experiment and mathematical modeling. The results of the investigation show that (i) a copper wire is coated under conditions of a.c. 50 Hz Joule heating in electrolyte containing 1.0 M $CuSO_4$ and 0.5 M H_2SO_4 with relatively high deposition rate of about 0.4 μm min^{-1}, (ii) the Joule heating current should be kept below the boiling point of the solution to realize uniform deposition, and (iii) results of calculations by the present model based on one-dimensional heat conduction agree well with experimental results.

Nomenclature

D	diameter of wire (m)
D_0	initial diameter of wire (m)
F	Faraday constant (96 487 C mol^{-1})
g	acceleration due to gravity (9.807 m s^{-2})
Gr	Grashof number
H	thickness of electrodeposit (m)
I	current (A)
i_0	exchange current density (A m^{-2})
i_n	current density normal to electode (A m^{-2})
J	current density ($\equiv I/S$) (A m^{-2})
L	length of wire (m)
M	molar concentration of electrolyte (mol dm^{-3} or M)
m	atomic weight (kg mol^{-1})
n	number of electrons participating
n	unit normal vector to boundary
Nu	Nusselt number
Pr	Prandtl number
q	heat per unit volume (W m^{-3})
R	universal gas constant (8.314 3 J mol^{-1} K^{-1})
(r, z)	cylindrical coordinate (m)
S	cross section of wire (m^2)
T	temperature (K)
T_0	fixed temperature at both ends of wire (K)
T_y	temperature of electrolyte (K)
t	time (s)
x	longitudinal coordinate over wire (m)

Greek symbols

α	heat transfer coefficient (W m^{-2} K^{-1})
$\alpha_{a,c}$	anodic (a) and cathodic (c) transfer coefficient
β	thermal expansion coefficient of solution (K^{-1})
γ	specific heat (J kg^{-1} K^{-1})
ϕ	potential (V)
ϕ_e	electrode potential (V)
λ	thermal conductivity (W m^{-1} K^{-1})
σ_y	ionic conductivity of electrolyte (Ω^{-1} m^{-1})
σ_e	electronic conductivity of electrode (Ω^{-1} m^{-1})
ν	kinematic viscosity (m^2 s^{-1})
η	surface overpotential ($\equiv \phi_e - \phi$) (V)
τ	time constant (s)
ρ	density (kg m^{-3})

1. Introduction

A unique self-induced repair (SIR) process utilizing thermal potential induced by Joule heating was reported by Chen [1] for repair of constrictions or incipient breaks in printed circuit boards. The method is essentially based on the 'thermal battery effect'. That is, if an electrode is locally heated in an electrolyte, a temperature difference is caused on the surface of the electrode and a thermal potential is generated at the interface between the electrode and the electrolyte. Since, in the case of a copper electrode, the hotter part corresponds to the cathode and the colder to the anode, copper is deposited at the hotter part of the electrode without requiring the application of an external d.c. voltage. The temperature difference serves as a d.c. power source for electrodeposition. When alternating current is applied to a copper wire with constrictions, the wire is locally heated at the constrictions as a result of Joule losses and copper is deposited so that the constrictions are repaired. The *IR* drop in the electrode due to a.c. current does not affect the deposition and the dissolution, because surface polarization is suppressed with applied a.c. voltage.

This process has the following advantages: (i) it is not necessary to know the exact location of defects, (ii)

* This work was presented at The 7th International Microelectronics Conference, Yokohama, Japan (1992).

0021-891X

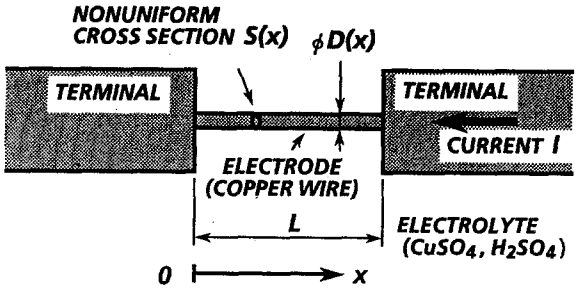

Fig. 1. One-dimensional model of Joule heating induced local electrodeposition.

the deposition continues until the temperature distribution becomes uniform over the wire, i.e. the process is self-terminating, (iii) plural defects in any one wire are simultaneously repaired without the need for any special controls, and (iv) chemical and structural integrity between the original wire and deposited copper can be achieved [1]. This process is expected to be applicable not only to the repair of incipient breaks in printed circuit boards but also to electrochemical deposition in the manufacturing of microelectronic devices and micromachines.

Although Chen [1] reported a fundamental experiment and a simple modeling of this process, both the experiment and the modeling were preliminary and only qualitative. In the present study a quantitative experiment was performed and a more detailed mathematical model was developed to clarify the mechanism of the process, and the utility of the model is demonstrated through comparison of simulated and experimental results.

2. Modeling

2.1. *Thickness of electrodeposition*

The geometric model employed both in the modeling and the experiment is shown in Fig. 1. Both ends of a fine copper wire of length L and diameter D are connected to relatively large terminals and an alternating current I is applied. The diameter of the copper wire is assumed to be nonuniform. The wire is immersed in electrolyte solution which contains cupric sulphate and sulphuric acid. The deposition thickness on the wire, H, is determined by Faraday's law.

$$\mathrm{d}H = \frac{m}{nF\rho} i_n \mathrm{d}t \tag{1}$$

The current density to the electrode, i_n, is approximately determined by the Butler–Volmer equation [7].

$$i_n = i_0 \left[\exp\left(\frac{\alpha_a F}{RT}\eta\right) - \exp\left(-\frac{\alpha_c F}{RT}\eta\right)\right] \tag{2}$$

Since, in the present system, the ohmic potential drop in the bulk electrolyte is negligible compared with the surface overpotential (see Appendix), the surface overpotential can be assumed to be equal to the electrode potential, ϕ_e, generated by the temperature difference on the surface of the electrode.

The temperature dependence of the potential was experimentally determined by Chen [1] to be a function of molar concentration of cupric sulphate, M_{CuSO_4}.

$$(\partial\phi_e/\partial T) = 0.675 \times 10^{-3} + 7.94 \times 10^{-5} \ln (M_{CuSO_4}) \tag{3}$$

Once the temperature distribution is determined, the other unknown variables, ϕ_e, i_n, and H, can be calculated by Equations 3, 2 and 1, in that order. Therefore, calculation of the temperature distribution over the electrode is essential to simulate the dynamics of the SIR process.

2.2. *Temperature distribution*

Because the diameter of the wire is very small compared with the length, the following one-dimensional time-dependent heat conduction equation describes the wire temperature distribution with Joule heating.

$$\rho\gamma \frac{\partial T}{\partial t} - \frac{\partial}{\partial x}\left(\lambda \frac{\partial T}{\partial x}\right) = \frac{J^2}{\sigma_e} - \alpha (T - T_y)\frac{4}{D} \tag{4}$$

The heat generated per unit volume of the wire, the right-hand side of Equation 4, is assumed to be by Joule heating (the first term of the right-hand side of Equation 4) minus the convective heat loss from the surface of the wire to the solution (the second term of the right-hand side of Equation 4). The heat transfer coefficient due to natural convection of the horizontal wire is calculated by the following formula [3].

$$235(Nu)^3 \exp(-6/Nu) = GrPr \tag{5}$$

Since the heat capacities of the negative and the positive terminals are large compared with that of the wire, the temperature at both ends of the wire is assumed to be constant.

$$T = T_0 \quad \text{at } x = 0, L \tag{6}$$

2.3. *Numerical method*

Equation 4 was numerically solved by the one-dimensional finite element method (FEM) and the Crank–Nicolson method under the boundary conditions (6)

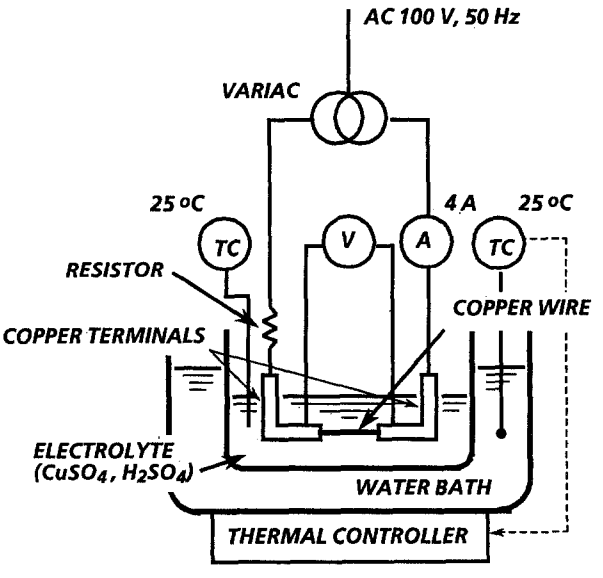

Fig. 2. Experimental setup.

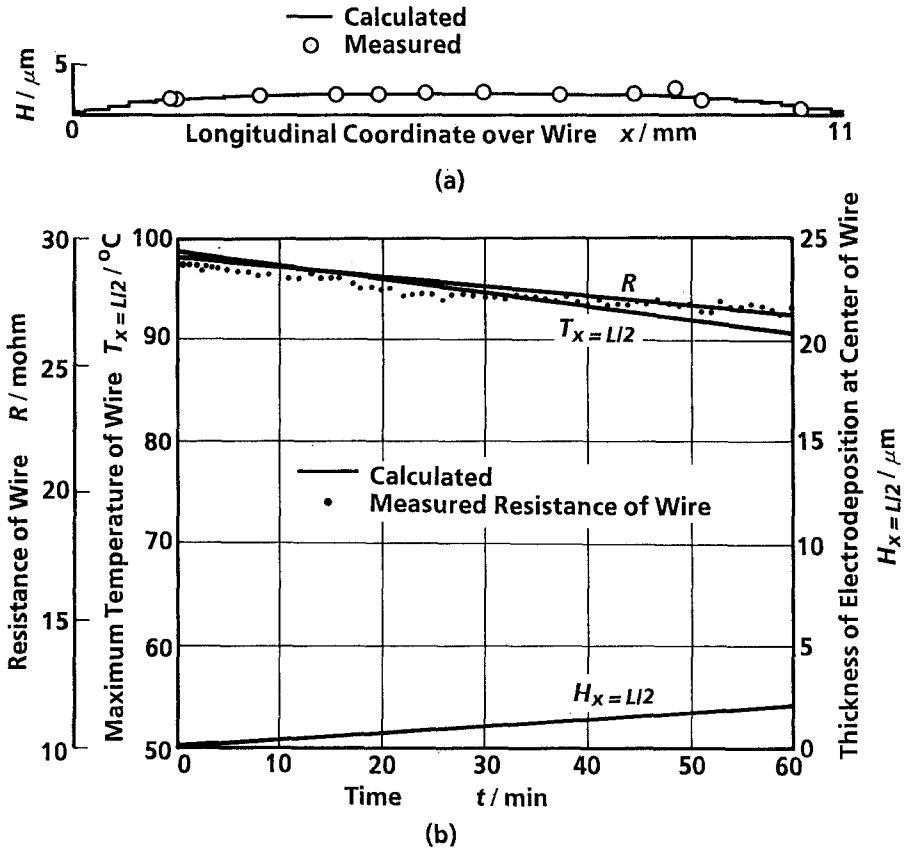

Fig. 3. Dynamics of Joule heating induced electrodeposition (Bath A). I = 4 A. (a) Distribution of deposited thickness after 60 min operation, (b) resistance, maximum temperature and deposited thickness during operation.

from an initial condition, $T(x, t = 0) = T_y$ [6]. The electrode potential, the normal current density, and the thickness of deposit at the designated time were then calculated in the order of Equations 3, 2 and 1, respectively. The temperature distribution for the next time step was then calculated with the revised diameter $D(x)$ $(= D_0 + 2H)$. Thermodynamic [4] and electrochemical [7] parameters of copper in $CuSO_4 - H_2SO_4$ solutions are available in the literature.

3. Experimental details

Figure 2 shows a schematic drawing of the experimental setup. The copper wire, initially 0.1 mm diameter and 1 mm length, was connected to the L-shaped copper terminals and immersed in electrolyte solution. Two kinds of electrolyte were employed for the experiments, Bath A containing 0.05 M $CuSO_4$, 1.0 M H_2SO_4, and Bath B containing 1.0 M $CuSO_4$, 0.5 M H_2SO_4. The temperature of the solution was kept constant at 25° C by a temperature-controlled water bath. 100 V at 50 Hz was used as the Joule heating power source, because it has been reported that the deposition process is independent of the frequency of the Joule heating current [1]. A variac was used to control the applied voltage, and a resistor was connected in series to assure virtually constant current even if the resistance of the wire changed during the operation. The a.c. voltage applied to the wire, the current, and the temperature of the electrolyte were monitored during the operation. The diameter of the wire before and after the experiment was measured by optical microscopy.

4. Results and discussion

4.1. *Dynamics of deposition*

Figures 3 and 4 show the results of experiments and calculations for Bath A and Bath B, respectively. The following points may be made.

(i) Initially, it was confirmed that copper was deposited with Joule heating in electrolyte solution without requiring the application of an external d.c. voltage as Chen [1] originally reported. In this experiment, the cool portions of the probe leads and the terminals acted as the anode and the source of copper deposited on the wire. However, the amount of copper deposition required for the SIR process is very small and, therefore, the amount of copper dissolution at the anode is also small [1].

(ii) When the operation was started, the wire heated up almost immediatlely, because the thermal time constant, τ, was small compared with the operating time. In the present system $\tau \approx \rho\gamma D/(4\alpha) \approx$ 0.07 s.

(iii) Copper was deposited to the wire in proportion to the temperature rise. As copper was deposited and the cross section of the wire increased, the Joule loss decreased and the temperature rise slowed. As a result, the deposition rate decreased gradually as the deposition progressed.

(iv) A higher deposition rate was realized with Bath

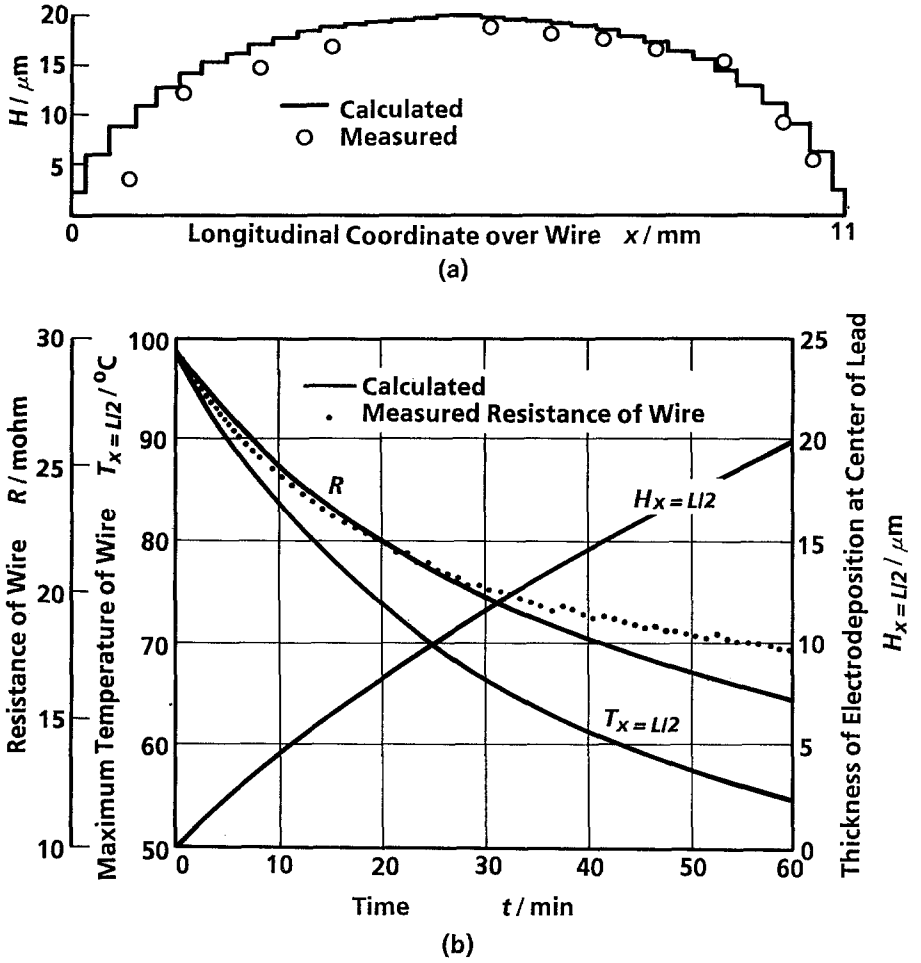

Fig. 4. Dynamics of Joule heating induced electrodeposition (Bath B). $I = 4$ A. (a) Distribution of deposited thickness after 60 min operation, (b) resistance, maximum temperature and deposited thickness during operation.

B, because both the thermal potential and the exchange current density in Bath B are larger than those in Bath A.* Since the maximum solubility of $CuSO_4$ in H_2O is 1.0 M at 20° C, the maximum temperature dependence of the thermal potential is 0.675 mV K^{-1} (Equation 3). On the other hand the exchange current density depends not only on M_{CuSO_4} but also $M_{H_2SO_4}$.† Though lower $M_{H_2SO_4}$ (Bath B) is preferable to realize high exchange current density (Equation 7), low concentration of the supporting electrolyte H_2SO_4 causes poor electrolyte conductivity and the increased *IR* drop in the bulk electrolyte may decrease the deposition rate (see Appendix). Therefore Bath B seems to be nearly optimum with respect to realizing high deposition rate.

(v) The initial deposition rate in Bath B was about 0.4 μm min^{-1} which is suitable for microelectronic applications.

(vi) The results of calculation using the present model agree reasonably well with the experimental results. However, the measured wire resistance in the case of Bath B was a little larger than the calculated value and thus the measured thickness of the electrodeposition was smaller than the calculated value. This discrepancy may be due to neglect of the *IR* drop in the electrolyte in the calculations. As quantitatively evaluated in the Appendix, since the normal current density to the wire neglecting the ohmic potential drop is about 14.5% larger than that in the resistive electrolyte (B), increased electrodeposition is calculated when the *IR* drop is neglected. The present model appropriately simulates the SIR process when the concentration of the supporting electrolyte, $M_{H_2SO_4}$, is larger than 0.5 M and thus the conductivity of the electrolyte is larger than 17.5 Ω^{-1} m^{-1}.

* The thermal potential multiplied by the exchange current density in Bath B is approximately 10 times larger than that in Bath A (see below).

Table 1. Electrochemical parameters of $CuSO_4$-H_2SO_4 solutions

Item	*Unit*	*Bath A*	*Bath B*	*Ref.*
$CuSO_4$ concentration	mol dm^{-3}	0.05	1.0	-
H_2SO_4 concentration	mol dm^{-3}	1.0	0.5	-
Ionic conductivity	Ω^{-1} m^{-1}	38.4	17.5	[7]
Temperature dependence of thermal potential	mV K^{-1}	0.620	0.675	[1]
Exchange current density	A m^{-2}	14.5	130	[7]

† The exchange current density was experimentally determined to be a function of M_{CuSO_4} and $M_{H_2SO_4}$ [7].

$$i_0 = 156(M_{CuSO_4})^{0.67} \exp\{-0.37(M_{H_2SO_4})\} \quad (7)$$

where i_0 is in A m^{-2}, and M_{CuSO_4} and $M_{H_2SO_4}$ are in mol dm^{-3}.

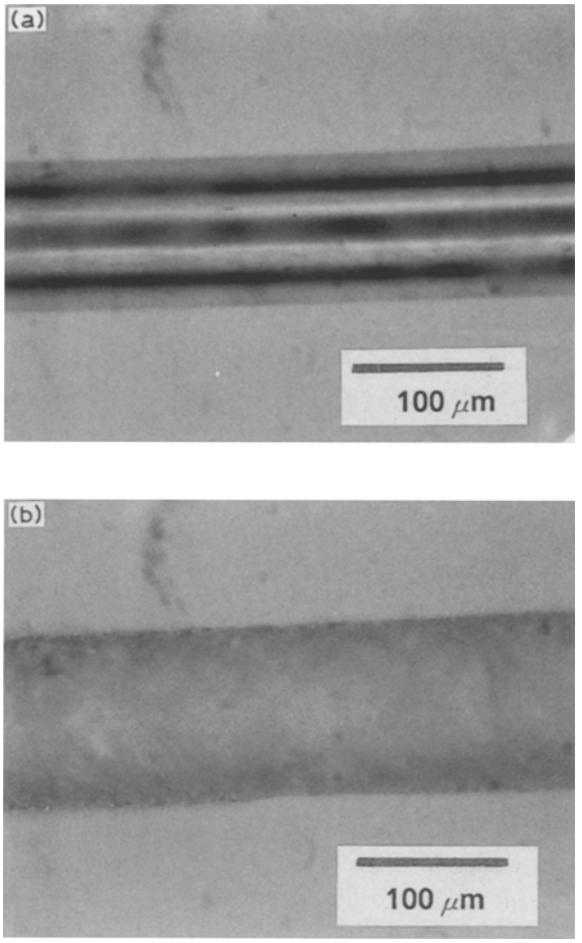

Fig. 5. Photographs of wires before and after 60 min operation in Bath B. (a) Before electrodeposition, $D = 100\,\mu m$, (b) after electrodeposition, $D = 136\,\mu m$.

4.2. *Limitation of deposition*

Figure 5 shows photographs of the wire before and after the operation in Bath B. Operating conditions were the same as those of Fig. 4. It is seen that the deposition was dense and continuous. On the other hand, Fig. 6 shows the photograph of the wire after 30 s operation with a current of 6 A in Bath B. The deposition rate was extremely high, which is partially attributed to the high thermal potential but mainly to the high mass transfer rate. That is, in addition to the high thermal potential, strong stirring of the solution due to the temperature gradient led to a high deposition rate as in laser enhanced electroplating [11–13]. With this current, however, the temperature of the solution adjacent to the wire exceeded its boiling point and bubbles were observed. Since bubbles form a barrier to ionic current passage, copper was not deposited at the parts covered with bubbles. The deposition surface, therefore, was rough and nonuniform. The current must be such that the boiling point of the solution is not exceeded to realize uniform and fine repair. For small constrictions, an increase in mass transfer rate and strong microstirring of the solution caused by thermal gradients and strong localized boiling results in an extremely high deposition rate without such nonuniformity, as Puippe *et al.* [13] observed in investigating laser-enhanced electroplating. However, for relatively large constrictions, boiling is not localized and causes nonuniform deposition as shown in Fig. 6. Thus, though a higher deposition rate than $0.4\,\mu m\,min^{-1}$ is possible for small constrictions, this value may be considered to be a maximum deposition rate for all size constrictions.

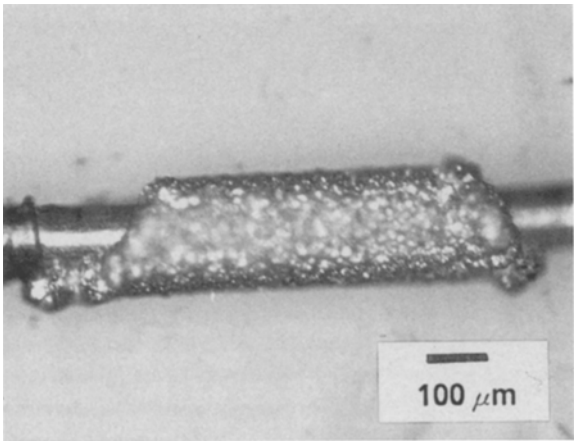

Fig. 6. Photograph of electrodeposited wire following the occurrence of boiling.

4.3. *Simulation of self-repair*

A series of numerical simulations on the self-induced repair process of constrictions was performed. Figure 7 shows examples of these calculations. Figure 7(a) shows the result of constant current operation at 1.2 A for 60 min. In the case of Fig. 7(b), on the other hand, the applied current was increased linearly from zero to 3 A for 30 min, i.e. at $0.1\,A\,min^{-1}$, and was then maintained at 3 A for an additional 30 min. The total operating time was 60 min, and the maximum temperature of the wire was 100° C for both (a) and (b). It is clearly seen that the constrictions were repaired in both cases, but the operating condition of case (b) achieved a higher deposition rate than in the constant current operation of case (a) [1]. A current increasing scheme is preferable to realize high deposition rate without the formation of bubbles.

5. Concluding remarks

(i) It is confirmed, as Chen [1] originally reported, that copper is electrodeposited using an a.c. Joule heating in an electrolyte solution which contains $CuSO_4$ and H_2SO_4 without requiring external d.c. power.

(ii) The dynamics of the deposition are (a) due to the small thermal time constant of the fine wire compared with the operating time, the lead heats up almost immediately, when a.c. current is applied, (b) copper deposits on the heated portion (cathode) of the wire and dissolves from the colder portion (anode) due to the thermal potential, (c) the Joule loss decreases with increase in the cross section at the heated part of the wire. This results in a decrease in the rate of temperature rise, (d) the deposition rate decreases gradually as

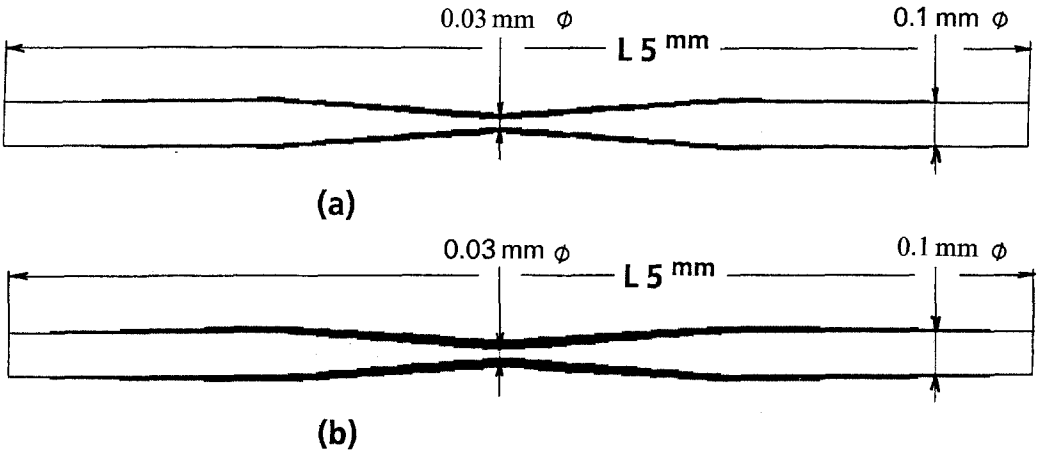

Fig. 7. Results of simulations for the self-induced repair process. (a) 1.2 A constant current operation for 60 min, (b) 0.1 A min^{-1} current increase scheme for 30 min and 3 A constant current operation for additional 30 min. While parts are the original wires with constrictions and black layers indicate deposited copper. Electrolyte: Bath B, temperature of bulk electrolyte: 25° C.

deposition increases, and then, (e) as the temperature over the wire becomes uniform, the deposition is self-terminating.

(iii) Higher deposition rate was realized with the solution of high concentration of $CuSO_4$ and low concentration of the supporting electrolyte, H_2SO_4, because both the thermal potential and the exchange current density are larger. A concentration of 1.0 M $CuSO_4$ and 0.5 M H_2SO_4 appeared optimum. The maximum deposition rate was about 0.4 $\mu m\ min^{-1}$, which is suitable for microelectronic applications.

(iv) Boiling of the solution due to an excess of applied a.c. current caused bubbles on the wire surface, which, in turn, caused non-unifrom deposition. The operation current must be controlled to keep the temperature below the boiling point of the solution.

(v) Relatively higher deposition rate was realized with a current increase mode of operation as compared with constant current operation.

(vi) Calculations using the present model, based on one-dimensional heat conduction, agree fairly well with the experimental results. The present model appropriately simulates the SIR process when the conductivity of the electrolyte is larger than 17.5 $\Omega^{-1} m^{-1}$.

Although this new and unique process was investigated and reported originally for repairing constrictions or incipient breaks on printed circuit boards, the process is expected to be applicable to the fine patterning of microelectronic devices, such as ionographic printing heads of printers or copiers [8]. Such applications are under investigation.

References

[1] C. J. Chen, *J. Electrochem. Soc.* **138** (1991) 969.
[2] H. Kawamoto, *J. Appl. Electrochem.* **22** (1992) 1113.
[3] W. Elenbass, *J. Appl. Phys.* **19** (1948) 1148.
[4] Japan Society of Mechanical Engineers (Edition), 'JSME Data Book: Heat Transfer; 4th edition', Japan Society of Mechanical Engineers (1986).
[5] J. S. Newman, 'Electrochemical Systems; 2nd Edition', Prentice-Hall, Englewood Cliffs, NJ (1991).
[6] H. Kawamoto and Y. Kusakabe, *J. Electrochem. Soc.* **136** (1989) 1355.
[7] R. Caban and T. W. Chapman, *ibid.* **124** (1977) 1371.
[8] SPIE – The International Society for Optical Engineering, 'Proceedings: Hard Copy Printing Technologies', **1252** (1990) p. 18.
[9] C. C. Zienkiewicz, 'The Finite Element Method'; 3rd edn., McGraw-Hill, New York (1977).
[10] F. A. Jagush, R. E. White and W. E. Ryan, *J. Electrochem. Soc.* **137** (1990) 1848.
[11] R. J. von Gutfeld, E. E. Tynan, R. L. Melcher and S. E. Bium, *Appl. Phys. Lett.* **35** (1979) 651.
[12] P. Bindra, G. V. Arbach and V. Stimming, *J. Electrochem. Soc.* **134** (1987) 2893.
[13] J. Cl. Puippe, R. E. Acosta and R. J. von Gutfeld, *ibid.* **128** (1981) 2539.

Appendix

Secondary current distribution

The adequacy of the assumption that the *IR* drop in the electrolyte is negligible as compared with the surface overpotential is assessed by calculating the secondary current distribution in a two-dimensional system. If it is assumed that the electrolyte is uniform and no concentration gradient exists, Laplace's equation applies in the electrolyte [2, 5].

$$\nabla^2 \phi = 0 \qquad \text{(A1)}$$

Figure 8 shows calculating conditions: (i) two-dimensional cylindrical coordinates (r, z) are employed, (ii) due to symmetry one half of the system is adopted for the calculation domain, and (iii) r_0 is large compared with the radius of the wire. Boundary conditions corresponding to the present system are

$$\phi = 0 \quad \text{at } r = r_0 \qquad \text{(A2)}$$

$$\boldsymbol{n} \cdot \nabla \phi = 0 \quad \text{at } z = 0,\ L/2 \qquad \text{(A3)}$$

$$\sigma_y \mathbf{n} \cdot \nabla \phi + i_0(\alpha_a + \alpha_c)F\phi/RT = i_0(\alpha_a + \alpha_c)F\phi_e/RT \quad \text{at } r = D/2 \qquad \text{(A4)}$$

Here, linear polarization [10] is assumed at the electrode surface, because the surface overpotential is small.

Equation A1 was numerically solved under linear boundary conditions A2, A3, and A4 with the finite element method with two-dimensional cylindrical coordinates [9]. Figure 9 shows the calculated secondary current distribution. The maximum potential drop in the Bath A is 0.9% of the maximum electrode

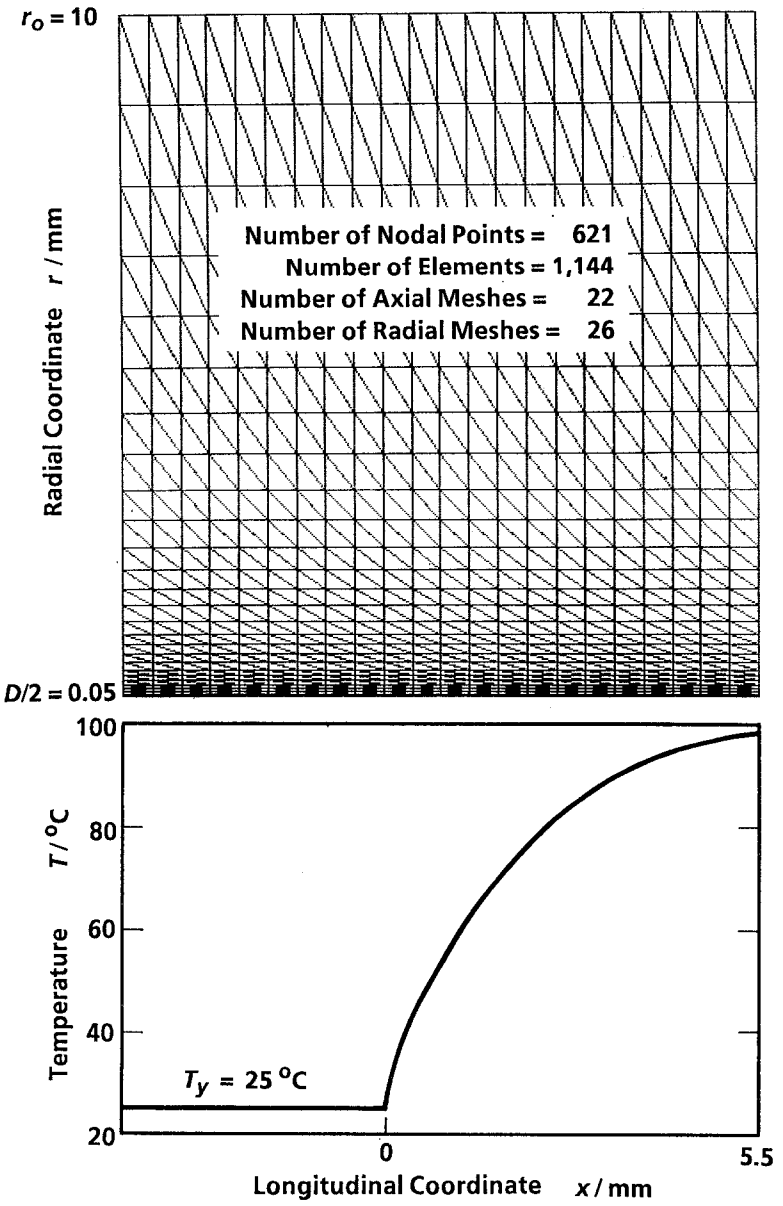

Fig. 8. Calculating conditions for secondary current distribution and mesh pattern for FEM calculation. The temperature distribution corresponds to the initial value just after 4 A current passage.

potential, whereas the maximum potential drop in Bath B is 14.5% of the maximum electrode potential. Figure 10 shows normal current density to the wire in the case of infinitely conductive electrolyte (neglect of electrolyte *IR* drop) and resistive electrolyte. It is apparent from the figure that the *IR* drop in the electrolyte is negligible in the highly conductive Bath A but substantial in the relatively resistive Bath B. The assumption of the neglect of *IR* drop is acceptable when the conductivity of the electrolyte is higher than $17.5\,\Omega^{-1}\,m^{-1}$.

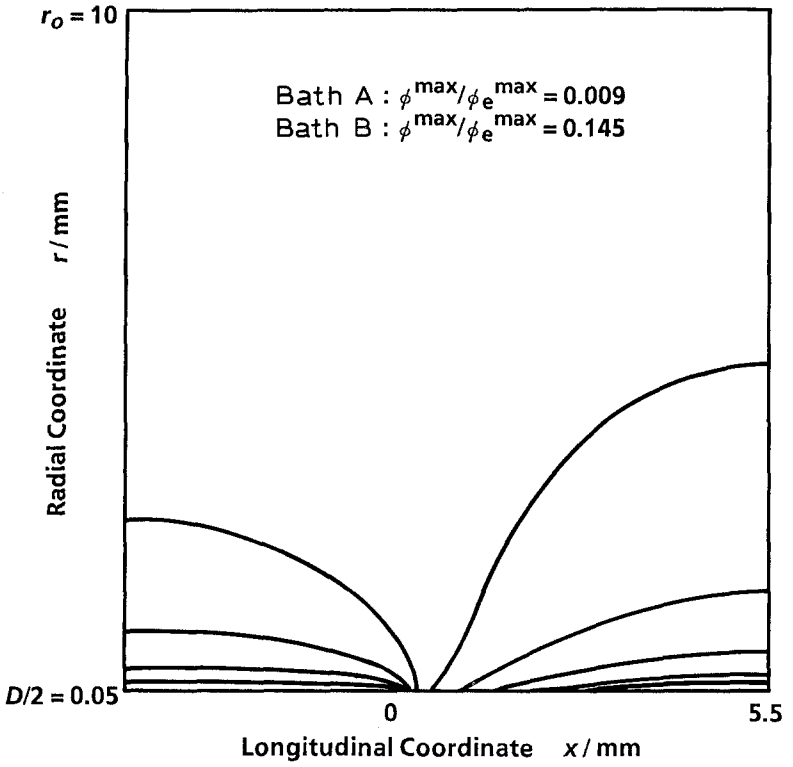

Fig. 9. Calculated secondary current distribution. Curves are equipotential surfaces designating to 10% of maximum potential drop in electrolyte. Common to both Bath A and Bath B.

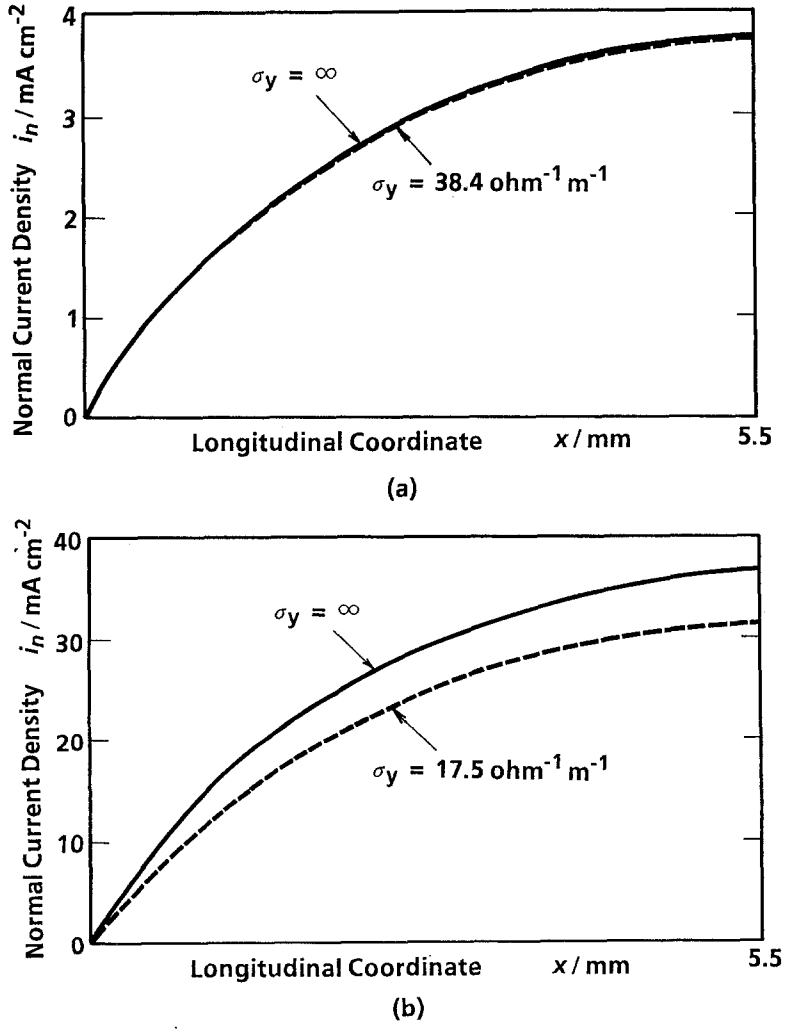

Fig. 10. Calculated normal current density to wire in infinitely conductive electrolyte and resistive electrolye. (a) In case of Bath A, (b) in case of Bath B.